Journal of Thrombosis and Haemostasis, **11**: 1399–1406 DOI: 10.1111/jth.12279

ORIGINAL ARTICLE

Crystal structure and enzymatic activity of an ADAMTS-13 mutant with the East Asian-specific P475S polymorphism

M. AKIYAMA,*[1] D. NAKAYAMA,*[1] S. TAKEDA,† K. KOKAME,* J. TAKAGI‡ and T. MIYATA*

**Department of Molecular Pathogenesis, National Cerebral and Cardiovascular Center; †Department of Cardiac Physiology, National Cerebral and Cardiovascular Center; and ‡Laboratory of Protein Synthesis and Expression, Institute for Protein Research, Osaka University, Osaka, Japan*

To cite this article: Akiyama M, Nakayama D, Takeda S, Kokame K, Takagi J, Miyata T. Crystal structure and enzymatic activity of an ADAMTS-13 mutant with the East Asian-specific P475S polymorphism. *J Thromb Haemost* 2013; **11**: 1399–406.

Summary. *Background:* An East Asian-specific P475S polymorphism in the gene encoding ADAMTS-13 causes an approximately 16% reduction in plasma ADAMTS-13 activity. *Objectives:* To demonstrate the impact of this dysfunctional polymorphism by characterizing the structure and activity of the P475S mutant protein. *Methods:* We determined the crystal structure of the P475S mutant of ADAMTS-13-DTCS (DTCS-P475S, residues 287–685) and compared it with the wild-type structure. We determined the enzymatic parameters of ADAMTS-13-MDTCS (residues 75–685) and MDTCS-P475S, and further examined the effects of denaturants and reaction temperature on their activity. We also examined the cleavage of shear-treated von Willebrand factor (VWF) by MDTCS-P475S. *Results:* MDTCS-P475S showed a reaction rate similar to that of wild-type MDTCS, but showed two-fold lower affinity for the peptidyl substrate, indicating that the Pro475-containing V-loop (residues 474–481) in the C_A domain is a substrate-binding exosite. Structural analysis showed that the conformation of the V-loop was significantly different in DTCS-P475S and the wild type, where no obvious interactions of Ser475 with other residues were observed. This explains the higher susceptibility of the enzymatic activity of MDTCS-P475S to reaction environments such as denaturants and high temperature. MDTCS-P475S can moderately cleave shear-treated VWF. *Conclusions:* We have provided structural evidence that the P475S polymorphism in ADAMTS-13 leads to increased local structural instability, resulting in lowered affinity for the substrate without changing the reaction rate. The moderate activity of ADAMTS-13-P475S for shear-treated VWF is sufficient to prevent thrombotic thrombocytopenic purpura (TTP) onset.

Keywords: ADAMTS-13, crystallography, genetic polymorphism, human, proteins, thrombotic thrombocytopenic purpura, von Willebrand factor.

Correspondence: Masashi Akiyama and Toshiyuki Miyata, Department of Molecular Pathogenesis, National Cerebral and Cardiovascular Center, 5-7-1 Fujishiro-dai, Suita, Osaka 565-8565, Japan.
Tel.: +81 6 6833 5012, ext: 2477 or 2512; fax: +81 6 6825 117.
E-mail: akiyamam@ri.ncvc.go.jp and miyata@ri.ncvc.go.jp

[1]These authors contributed equally to this work.

Received 11 October 2012
Manuscript handled by: D. Lane
Final decision: D. Lane, 5 April 2013

Introduction

von Willebrand factor (VWF) is a plasma glycoprotein synthesized primarily in vascular endothelial cells and megakaryocytes [1]. VWF is released into plasma as ultralarge multimeric forms (ultralarge VWF [UL-VWF]) that are highly active in platelet aggregation. ADAMTS-13 specifically cleaves the Tyr1605–Met1606 bond within the A2 domain of VWF in a fluid shear stress-dependent manner, and controls platelet thrombus formation [2,3]. Severe deficiency in ADAMTS-13 activity, caused by either genetic mutations or acquired autoantibodies against ADAMTS-13, results in the accumulation of UL-VWF in plasma, which leads to the hyperaggregation of platelets. This prothrombotic condition can cause thrombotic thrombocytopenic purpura (TTP) [4].

The human *ADAMTS13* gene encodes a precursor protein of 1427 amino acids with a modular structure consisting of a signal peptide, a propeptide, a metalloprotease (M) domain, a disintegrin-like (D) domain, a thrombospondin type 1 repeat (TSR) (T1), a cysteine-rich (C) domain, a spacer (S) domain, seven TSRs (T2–T8), and two CUB domains [5–7]. In addition to the causative mutations for TTP, a number of missense mutations and polymorphisms have been identified in *ADAMTS13* [6,8,9]. Among them, P475S (c.1423C>T) is a dysfunctional missense polymorphism with a minor allele frequency of 5.0% [8,10]. Subjects carrying the minor

allele residue (serine) showed ~ 16% lower ADAMTS-13 activity than those without the polymorphism. The P475S polymorphism has also been identified in Koreans (allele frequency of 4.0%) [11] and Chinese (1.5%) [12], but is absent in Caucasians [13], suggesting that ADAMTS-13-P475S is an East Asian-specific natural dysfunctional mutant [14]. An in vitro study demonstrated that ADAMTS-13-P475S is normally secreted from cultured cells. However, the culture medium containing ADAMTS-13-P475S showed greatly reduced enzymatic activity (~ 10%) in the VWF multimer assay [8]. On the other hand, partially purified ADAMTS-13-P475S showed ~ 70% of wild-type activity in an assay with a synthetic peptidyl fluorogenic substrate, FRETS-VWF73 [15]. The difference in enzymatic activity of ADAMTS-13-P475S between the two assays was probably attributable to the presence and absence of urea in the reaction mixture [15]. These experiments were performed with ADAMTS-13-containing culture medium or partially purified ADAMTS-13; therefore, analysis of enzyme kinetics with the purified protein remains to be performed.

Several studies have indicated that ADAMTS-13-MDTCS has VWF-cleaving activity that is nearly identical to that of full-length ADAMTS-13 in vitro [16,17]. We recently determined the crystal structures of ADAMTS-13-DTCS [18]. The C domain was further divided into the globular C_A domain and elongated C_B domain. Extensive structure-based mutagenesis indicated that ADAMTS-13 can bind to VWF through at least three VWF-binding exosites on the linearly aligned discontinuous surfaces of the D, C_A and S domains [18], and this substrate-binding mode with multiple binding sites is supported by other studies [19–22]. The Pro475 in question is located in the V-loop (residues 474–481) of the C_A domain. Mutations in the V-loop of the C_A domain resulted in significantly reduced enzymatic activity, suggesting that the V-loop creates a VWF-binding exosite [18].

In this study, we determined the crystal structure of DTCS-P475S, and characterized the enzymatic activity of MDTCS-P475S. The present study provides evidence that the P475S substitution in ADAMTS-13 destabilizes the local conformation of the V-loop in the C_A domain, resulting in lowered substrate affinity without changing the reaction rate. Furthermore, the moderate cleavage of shear-treated VWF by ADAMTS-13-P475S suggests that the VWF-cleaving activity of the mutant is sufficient to prevent TTP onset.

Materials and methods

Preparation, crystallization and structural analysis of DTCS-P475S

Production of DTCS-P475S was performed with a previously described method [23], with some modifications. Briefly, a stable cell line (HEK293S GnTI$^-$ cells) [24] secreting DTCS-P475S (residues 287–685) with a C-terminal tobacco etch virus (TEV) proteinase cleavage site followed by tandem His-tag sequences was selected and cultured. The culture medium was first concentrated with 50% (w/v) ammonium sulfate, and DTCS-P475S was purified by Ni^{2+}–nitrilotriacetic acid (NTA) agarose column chromatography (Sigma-Aldrich, St Louis, MO, USA). After digestion with TEV proteinase, DTCS-P475S was further purified with a Resource S cation-exchange column (GE Healthcare, Hatfield, UK), concentrated to 10 mg mL^{-1}, and crystallized in 20% (w/v) poly(ethylene glycol) 1500 and 100 mM Mes (pH 6.0), with the same method as described for wild-type DTCS [23]. The diffraction data were collected at the SPring-8 beamline BL38B1 by use of a Rayonix MX225HE CCD detector with a wavelength of 1.0 Å at 100 K. The structure of DTCS-P475S was solved with the molecular replacement method, with the MOLREP program of the CCP4 suite [25], and the structure of wild-type DTCS (Protein Data Bank [PDB] ID: 3GHM) as a starting model. After manual rebuilding with COOT [26], the model was refined with the REFMAC program in CCP4 [25] and CNS [27]. Data collection and refinement statistics are summarized in Table S1. Figures were generated with the PYMOL Molecular Graphics System (Version 1.5; Schrödinger, LLC, Boston, MA, USA). The atomic coordinates of DTCS-P475S have been deposited in the PDB (ID: 3VN4).

Expression and purification of MDTCS and MDTCS-P475S

Recombinant MDTCS and MDTCS-P475S (residues 75–685) were expressed in CHO Lec 3.2.8.1 cells [23] with a BelloCell Cell Culture System (CESCO Bioengineering, Taichung, Taiwan). After 50% (w/v) ammonium sulfate precipitation of the culture medium, MDTCS and MDTCS-P475S were each purified with an Ni^{2+}–NTA column followed by a Resource S cation-exchange column. Both recombinant proteins, when resolved on an SDS–polyacrylamide gel and stained with Coomassie Brilliant Blue, showed a single band of molecular mass 74 kDa, which coincided well with the molecular mass of 75 kDa estimated from their sequences. The protein concentration was determined by use of the 660-nm Protein Assay Reagent (Thermo Fisher Scientific, Waltham, MA, USA) with bovine serum albumin as a protein concentration standard, and adjusted to 1.8 nM in 10 mM Hepes (pH 7.4), 150 mM NaCl, 0.005% Tween-20, and 50% glycerol.

Kinetic analysis of FRETS-VWF73 cleavage by MDTCS and MDTCS-P475S

The kinetic parameters of MDTCS and MDTCS-P475S were determined with FRETS-VWF73 (Peptide Institute, Minoh, Japan), as described previously [28,29]. FRETS-VWF73 (0–4 μM) was incubated with 0.18 nM MDTCS or MDTCS-P475S in 10 mM Hepes (pH 7.4), 150 mM NaCl

and 0.005% Tween-20 at 37 °C. Fluorescence intensities were measured with the M × 3000p QPCR System (Agilent Technologies, Santa Clara, CA, USA) equipped with 340-nm excitation and 450-nm emission filters. The reaction rate was calculated by linear regression analysis of fluorescence over time from 0 to 60 min with PRISM 5 software (GraphPad Software, La Jolla, CA, USA). To obtain the reaction rate, various amounts of FRETS-VWF73 (5, 10, 20 and 50 μmol) were completely cleaved with 10 nM ADAMTS-13-MDTCS for 90 min, and their fluorescence intensities were used to estimate the amount of cleaved product (Fig. S1). The reaction rates as a function of substrate concentration were fitted to the Michaelis–Menten equation, and the maximum velocity (V_{max}), the rate constant (k_{cat}) and the affinity (K_m) were calculated with PRISM 5.

Cleavage of shear-treated VWF by MDTCS and MDTCS-P475S

The cleavage of shear-treated VWF by ADAMTS-13 was performed as described previously [30], with some modifications. Briefly, purified plasma VWF (25 μg mL^{-1}, 100 nM VWF monomers) [31] was vortexed at a rotation rate of 2500 r.p.m. for the indicated times in 10 mM Hepes (pH 7.4), 150 mM NaCl and 0.005% Tween-20 at 24 °C on a digital vortex mixer (Scientific Industries, Bohemia, NY, USA). MDTCS or MDTCS-P475S (1 nM each) was added to the VWF solution and incubated for the indicated times at 37 °C. The digested samples were separated by SDS-PAGE under reducing conditions, and transferred to a poly(vinylidene difluoride) membrane. The cleavage products were detected by western blotting with horseradish peroxidase-conjugated anti-VWF polyclonal antibody (Dako, Carpinteria, CA, USA) and the Luminata Forte Chemiluminescent Reagent (Millipore, Billerica, MA, USA). The band intensities of the cleavage products (150 kDa) were quantified with MULTI GAUGE software (Fuji Film, Tokyo, Japan).

Effects of denaturants and temperature on FRETS-VWF73 cleavage by MDTCS and MDTCS-P475S

MDTCS or MDTCS-P475S (1 nM each) was mixed with 1 μM FRETS-VWF73 in 10 mM Hepes (pH 7.4), 150 mM NaCl and 0.005% Tween-20 containing urea (0–2.5 M) or guanidine-HCl (0–0.5 M), and incubated for 2 min at 37 °C; the fluorescence intensities were then measured at 37 °C for 60 min. To investigate the effects of reaction temperature, the cleavage reaction mixtures were incubated for 2 min at 37, 40, 45 and 50 °C, and the fluorescence intensities were then measured for 60 min at the respective temperatures. The reaction rate was calculated by performing linear regression analysis of the plot of fluorescence against time from 0 to 60 min with PRISM 5.

Results

Crystal structure of DTCS-P475S

The overall structure of DTCS-P475S refined at 2.8-Å resolution is shown in Fig. 1A. The structure includes ADAMTS-13 residues 298–324, 328–458, and 466–682. The backbone structure of DTCS was very similar to the previously solved wild-type DTCS structure [18], with an overall root mean square deviation of 0.421 Å for 369 Cα atoms (Fig. 1B). The electron densities associated with the V-loop (Val474–Ala481) were clearly observed in the current DTCS-P475S structure (Fig. 1C), enabling a detailed structural comparison between the wild type and the mutant. The conformation of the V-loop in the C_A domain of DTCS-P475S was significantly different from that in two previously determined DTCS structures. In DTCS, an oxygen atom in the main chain of Pro475 formed hydrogen bonds with the side chains of Ser477 and Gln478, the distances of which were 3.5 Å/3.8 Å and 3.1 Å/3.5 Å, respectively (calculated from two DTCS structures) (PDB ID: 3GHM/3GHN) (Fig. 1D). On the other hand, these distances in DTCS-P475S were 5.0 Å and 8.3 Å, respectively (Fig. 1E). In the DTCS structure, Pro475 also formed van der Waals contacts with Met509 in the C_A domain (3.8 Å/3.5 Å) and with Leu620 in the β6–β7 loop of the S domain (3.5 Å/4.0 Å), and stabilized the structure (Fig. 1D). The distances between Ser475 and Met509 (7.1 Å), and between Ser475 and Leu620 (5.1Å), were longer in DTCS-P475S than in DTCS, where the interactions no longer occurred (Fig. 1E). The lack of obvious interactions of Ser475 with other residues in the C_A and S domains in DTCS-P475S suggests that the V-loop structure is less stable in DTCS-P475S than in DTCS. The structures of the other loops in the C_A domain of DTCS-P475S did not differ significantly from those of DTCS.

Electron densities for the carbohydrate moieties of two potential *N*-linked sites (Asn552 and Asn614) and a potential *O*-linked site (Ser399) were present in both DTCS-P475S and DTCS [18]. An electron density linked to the side chain of Trp387 in the T1 domain was detected in DTCS-P475S (Fig. 1F). Trp387 is a conserved *C*-mannosylation site (WXXW, where the first tryptophan would be glycosylated), and *C*-mannosylation has been observed on conserved tryptophan residues in a number of TSRs [32], including ADAMTS-5 [33], suggesting that Trp387 is possibly *C*-mannosylated, although this modification was not clear in the electron densities of wild-type DTCS structures. In *C*-mannosylation, a mannose group is added to the C2 atom of the tryptophan.

Kinetic parameters of MDTCS and MDTCS-P475S

We measured the ADAMTS-13 activities of MDTCS and MDTCS-P475S with FRETS-VWF73, and determined their kinetic parameters. The cleavage reaction was monitored as

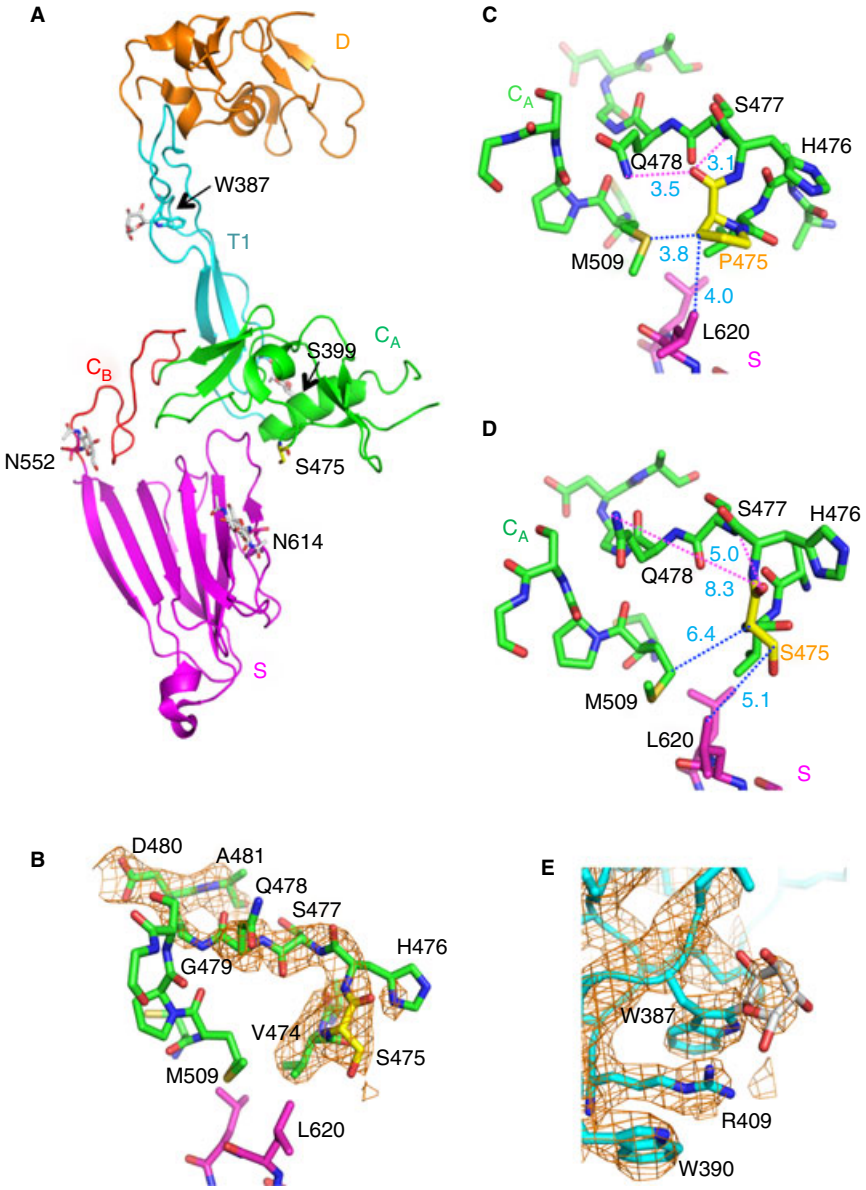

Fig. 1. Crystal structure of DTCS-P475S. (A) Overall structure of DTCS-P475S. Potential *N*-glycosylation at Asn552 (in the C_B domain) and Asn614 (in the S domain), *O*-fucosylation at Ser399 (in the T1 domain), and *C*-mannosylation at Trp387 (in the T1 domain) are shown as stick models. D, orange; T1, cyan; C_A, green; C_B, red; S, magenta. (B) A $2F_o - F_c$ electron density map (contoured at 1.2σ) associated with the V-loop in the C_A domain of DTCS-P475S. (C, D) Close-up view around the V-loop of the C_A domain in DTCS (C) and DTCS-P475S (D). The magenta and blue dotted lines show the hydrogen bonds and van der Waals contacts, respectively, of Pro475 in DTCS (C, PDB ID: 3GHN). For comparison, the corresponding lines are also shown in DTCS-P475S (D). The blue numbers show the distances between the atoms (Å). (E) A $2F_o - F_c$ electron density map (contoured at 1.2σ) is associated with the carbohydrate moiety linked to Trp387, most likely mannose.

an increase in the fluorescence of cleaved FRETS-VWF73, and converted to the reaction rate. The reaction showed typical Michaelis–Menten kinetics (Fig. 2). The V_{max} values of MDTCS and MDTCS-P475S were the same (0.35 nM s^{-1}), and their k_{cat} values were similar (MDTCS, 1.94 ± 0.08 s^{-1}; MDTCS-P475S, 1.90 ± 0.11 s^{-1}; Table 1). On the other hand, the K_m of MDTCS-P475S (0.82 ± 0.12 μM) was two-fold higher than that of MDTCS (0.37 ± 0.06 μM). These results indicated that the P475S substitution in MDTCS resulted in a two-fold reduction in catalytic efficiency (k_{cat}/K_m), mainly because of its lower affinity for FRETS-VWF73. We performed a thermal shift assay involving MDTCS and MDTCS-P475S by using SYPRO Orange (Fig. S2). The T_m values of MDTCS and MDTCS-P475S were identical in the absence (50 °C) and presence (46 °C) of 1.5 M urea.

Shear-treated VWF cleavage by MDTCS and MDTCS-P475S

As the scissile Tyr1605–Met1606 bond of VWF is buried within the core of the globular A2 domain [34], VWF under static conditions is not a good substrate for ADAMTS-13.

Table 1 Michaelis–Menten kinetic parameters of MDTCS and MDTCS-P475S

	MDTCS	MDTCS-P475S
K_m (μM)	0.37 ± 0.06	0.82 ± 0.12
k_{cat} (s^{-1})	1.94 ± 0.08	1.90 ± 0.11
k_{cat}/K_m (μM^{-1} s^{-1})	5.26 ± 0.52	2.32 ± 0.67
V_{max} (nM s^{-1})	0.35 ± 0.02	0.35 ± 0.02

Values are means ± standard deviation.

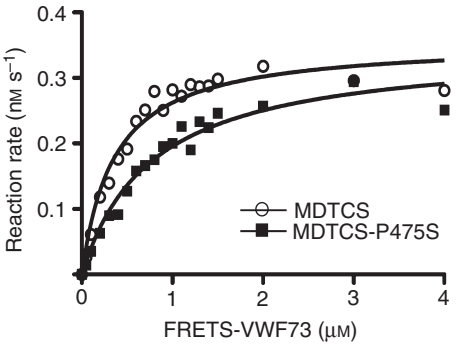

Fig. 2. Kinetic analysis of the cleavage of FRETS-VWF73 by MDTCS and MDTCS-P475S. FRETS-VWF73 (0.05–4 μM) was incubated with MDTCS (open circles, 0.18 nM) or MDTCS-P475S (closed squares, 0.18 nM) at 37 °C. The reaction rate was obtained from the increase in fluorescence over time. The line represents the non-linear fit to the Michaelis–Menten equation. VWF, von Willebrand factor.

When VWF is subjected to shear stress in circulation in vivo or denaturants in vitro, the A2 domain unfolds and adopts a partially extended conformation that makes its scissile peptide bond accessible for cleavage by ADAMTS-13 [19,35]. VWF treated with mechanistic-induced flow on a vortex mixer can be easily cleaved by ADAMTS-13 [30], so this fluid shear-treated VWF-cleaving assay is useful for the investigation of ADAMTS-13 function and regulation. We examined the activities of MDTCS and MDTCS-P475S against shear-treated VWF. VWF cleavage was monitored by the appearance of the 150-kDa band on western blotting with the anti-VWF antibody. Although both MDTCS and MDTCS-P475S produced the 150-kDa fragment band after a 10-min incubation, the band intensity was weaker for MDTCS-P475S (63% ± 8.2% at 120 min) than for MDTCS (Fig. 3A). Shearing treatment of MDTCS-P475S did not affect VWF-cleaving activity (Fig. 3B). These results suggest that MDTCS-P475S moderately cleaves VWF, once the scissile bond in VWF is exposed by shear stress. Shear treatment-induced cleavage of VWF by MDTCS-P475S was more severely inhibited than that by MDTCS upon the addition of urea. The VWF-cleaving activities of MDTCS and MDTCS-P475S in the presence of 1.5 M urea were 47.0% ± 6.5% and 8.9% ± 1.9%, respectively (Fig. 3C).

Effects of denaturants and temperature on the enzymatic activities of MDTCS and MDTCS-P475S

As the addition of urea severely inhibited the shear-dependent cleavage of VWF by MDTCS-P475S, we examined the effects of denaturants on the activity of MDTCS and MDTCS-P475S by using FRETS-VWF73. The reaction rates of MDTCS and MDTCS-P475S were

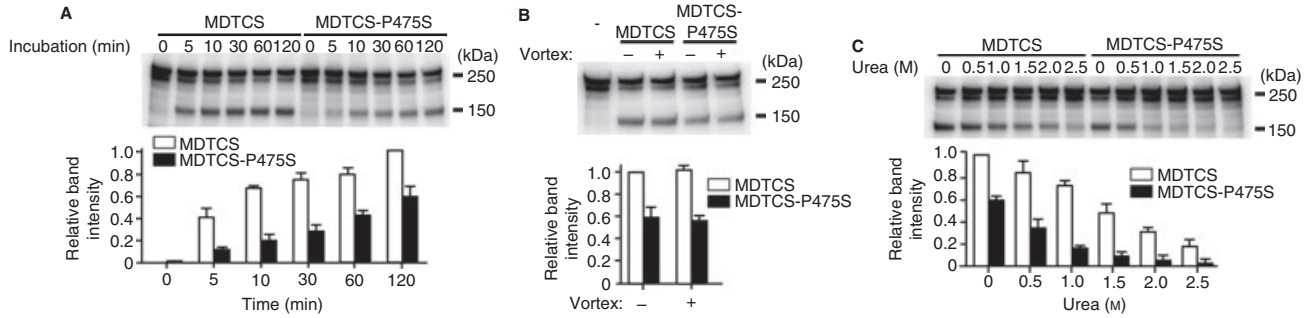

Fig. 3. Cleavage of shear-treated von Willebrand factor (VWF) by MDTCS and MDTCS-P475S. (A) Top: western blotting image showing VWF cleavage at each time point. The VWF multimer (25 μg mL^{-1}; 100 nM VWF monomers) was treated with shear with a 3-min vortex at 2500 r.p.m. at 24 °C, and MDTCS or MDTCS-P475S (1 nM) was then added to the reaction mixture. After incubation for the indicated times (0–120 min) at 37 °C, VWF cleavage was detected by the appearance of the 150-kDa band on western blotting with the anti-VWF antibody. Bottom: densitometric analysis of VWF cleavage. The band intensities of the cleavage products (150 kDa) were quantified as described in Materials and Methods. Band intensities relative to that of MDTCS at 120 min (set as 1) were plotted as means ± standard deviation (n = 3). (B) Top: western blotting image showing VWF cleavage by shear-treated or untreated MDTCS or MDTCS-P475S. The VWF multimer (25 μg mL^{-1}) was treated by shearing with vortexing for 3 min, and MDTCS or MDTCS-P475S (1 nM each), treated with shearing (2500 r.p.m. for 10 min), was then added to the reaction mixture. After incubation for 120 min at 37 °C, the cleavage of shear-treated VWF was detected as described in (A). Bottom: densitometric analysis of VWF cleavage. Band intensities relative to that of MDTCS without vortex (set as 1) were plotted as means ± standard deviation (n = 3). (C) Top: western blotting image showing VWF cleavage at various concentrations of urea. The VWF multimer (25 μg mL^{-1}) was treated with shear with a 3-min vortex, and MDTCS or MDTCS-P475S (1 nM each) was then added to the reaction mixture containing 0–2.5 M urea. After incubation for 120 min at 37 °C, the cleavage of shear-treated VWF was detected as described in (A). Bottom: densitometric analysis of VWF cleavage. Band intensities relative to that of MDTCS at 0 M urea (set as 1) were plotted as means ± standard deviation (n = 3).

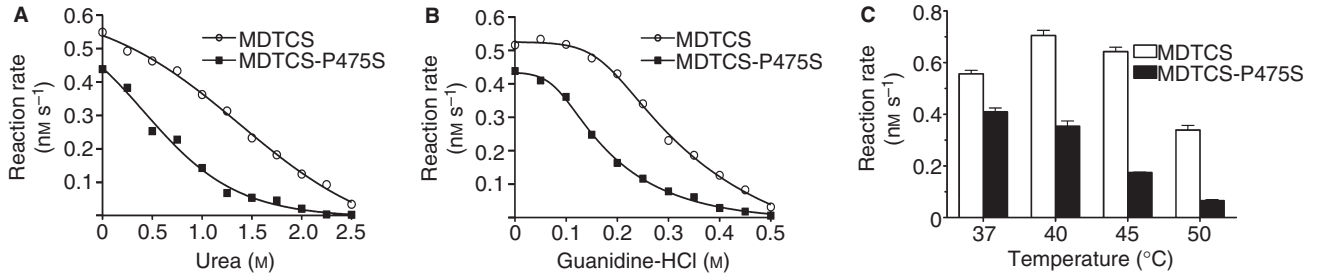

Fig. 4. Effects of denaturants and temperature on the FRETS-VWF73-cleaving activity of MDTCS and MDTCS-P475S. The enzymatic activities of MDTCS and MDTCS-P475S (0.8 nM) were measured for 60 min by the use of FRETS-VWF73 (1 μM) in the presence of urea (A) or guanidine-HCl (B) at 37 °C, or at different reaction temperatures (C). Values are means ± standard deviation (C: $n = 3$). VWF, von Willebrand factor.

reduced according to the concentrations of urea (Fig. 4A) or guanidine-HCl (Fig. 4B). The half-maximal inhibitory concentration (IC_{50}) for urea was 1.5 M for MDTCS and 0.8 M for MDTCS-P475S. The IC_{50} for guanidine-HCl was 0.3 M for MDTCS and 0.15 M for MDTCS-P475S. Furthermore, the activities of MDTCS and MDTCS-P475S were measured at 37, 40, 45 and 50 °C (Fig. 4C). A higher reaction temperature caused a more severe decrease in the activity of MDTCS-P475S than of MDTCS.

Discussion

Racial or ethnic group-specific genetic factors are now recognized to be important factors in the pathogenesis of thrombosis [36,37]. We previously identified the dysfunctional P475S polymorphism in ADAMTS-13 [8], and showed that it is East Asian-specific [14]. In the present study, we demonstrated that MDTCS-P475S showed moderate cleavage activity against shear-treated VWF, suggesting that the P475S polymorphism is not a causative factor in the development of TTP. However, this does not exclude the possibility that the P475S polymorphism could increase the risk for acquired TTP caused by inhibitory autoantibodies against ADAMTS-13. The relationship of the P475S polymorphism with acquired TTP remains to be addressed.

Recent studies have indicated the important function of the D and S domains as substrate-binding exosites [19–21]. We have identified at least three putative VWF-binding exosites, within the D, C_A and S domains, linearly aligned in the three-dimensional structure [18]. In the present study, kinetic analysis with FRETS-VWF73 showed that the lower catalytic efficiency (k_{cat}/K_m) of MDTCS-P475S was caused by lower affinity (higher K_m) but not by lower catalytic activity (lower k_{cat}). This also supports the idea that the V-loop in the C_A domain is a VWF-binding exosite.

The thermal shift assay showed that the thermostabilities of MDTCS and MDTCS-P475S were almost the same. Although the interaction between Ser475 in the V-loop of the C_A domain and Leu620 in the β6–β7 loop of the S domain was disrupted in the MDTCS-P475S structure, van der Waals contacts between Leu621 in the S domain and a hydrophobic pocket in the C_A domain formed by Gln442, Leu443, Met446, Val474, Arg507, Cys508 and Met509 [18] were retained. These interactions may minimize the adverse effect of P475S substitution on the stability of the S domain. These observations suggest that the reduction in the activity of MDTCS-P475S is not a consequence of global protein instability, but rather of a reduction in the enzyme–substrate interaction owing to the local conformational change in the V-loop (especially interatomic interactions with Ser475) (Fig. 1D). The greatly reduced enzymatic activity of MDTCS-P475S in the presence of urea and at a higher reaction temperature suggests that the P475S substitution induces a more severe local conformational change in the V-loop under these conditions and reduces the enzyme–substrate interaction.

Pro475 is conserved in all primates examined but not in other species (Fig. S3). Mouse ADAMTS-13 shows significantly reduced enzymatic activity against human VWF [38], indicating the species specificity of the ADAMTS-13–VWF interaction. Several amino acids in the core binding region for ADAMTS-13 in the A2 domain of VWF (VWF73) [39] differ among species (Fig. S4). Nonconserved amino acids in the exosites of ADAMTS-13 and in the VWF73 region of VWF may have coevolved for species-specific ADAMTS-13–VWF interface recognition.

Post-translational protein *C*-mannosylation is the attachment of an α-mannopyranosyl residue to the indole C-2 of tryptophan via a C–C linkage [32]. Proteins known to be *C*-mannosylated are RNase, interleukin-12, the mucins MUC5AC and MUC5B, and several proteins containing TSRs, such as thrombospondin-1, F-spondin, C6, C7, properdin, ADAMTS-L1, and ADAMTS-5 [33]. In the present study, potential *C*-mannosylation of Trp387 in the T1 domain of ADAMTS-13 has been suggested for the first time. *C*-mannosylation typically occurs in TSRs within the sequence motif W*XX*W, which is highly conserved among ADAMTS family members (ADAMTSs and ADAMTS-Ls) [33]. The functional role of *C*-mannosylation in ADAMTS-13 is unknown; however, a *C*-

mannosylation defect in ADAMTS-L1 decreases its secretion, suggesting a role in the regulation of protein secretion [33].

Addendum

M. Akiyama, D. Nakayama, and S. Takeda: performed research, analyzed data, and wrote the manuscript; K. Kokame: designed the experiments; J. Takagi: provided laboratory reagents; T. Miyata: wrote the manuscript and provided funding. All authors have approved the final draft.

Acknowledgements

The authors thank Y. Fujimura at Nara Medical University for providing us with purified plasma VWF. We also thank T. Kunieda for her help with protein purification, and M. Tomisako for her help with crystallization. This work was supported by grants-in-aid from the Ministry of Health, Labor, Welfare of Japan, the Ministry of Education, Culture, Sports, Science and Technology of Japan, and the SENSHIN Medical Research Foundation.

Disclosure of Conflict of Interests

The authors state that they have no conflict of interest.

Supporting Information

Additional Supporting Information may be found in the online version of this article:

Figure S1. Calibration curves for FRETS-VWF73 cleavage.
Figure S2. Thermal shift assay profiles of MDTCS and MDTCS-P475S.
Figure S3. Amino acid sequence alignment of the C_A domain of ADAMTS-13 from different species.
Figure S4. Amino acid sequence alignment of the core binding region for ADAMTS-13 in the A2 domain of VWF from different species.
Table S1. Data collection and refinement statistics.

References

1 Springer TA. Biology and physics of von Willebrand factor concatamers. *J Thromb Haemost* 2011; **9**(Suppl. 1): 130–43.
2 Dent JA, Galbusera M, Ruggeri ZM. Heterogeneity of plasma von Willebrand factor multimers resulting from proteolysis of the constituent subunit. *J Clin Invest* 1991; **88**: 774–82.
3 Tsai HM, Sussman II, Nagel RL. Shear stress enhances the proteolysis of von Willebrand factor in normal plasma. *Blood* 1994; **83**: 2171–9.
4 Sadler JE, Moake JL, Miyata T, George JN. Recent advances in thrombotic thrombocytopenic purpura. *Hematology Am Soc Hematol Educ Program* 2004; **2004**: 407–23.
5 Soejima K, Mimura N, Hirashima M, Maeda H, Hamamoto T, Nakagaki T, Nozaki C. A novel human metalloprotease synthesized in the liver and secreted into the blood: possibly, the von Willebrand factor-cleaving protease? *J Biochem* 2001; **130**: 475–80.
6 Levy GG, Nichols WC, Lian EC, Foroud T, McClintick JN, McGee BM, Yang AY, Siemieniak DR, Stark KR, Gruppo R, Sarode R, Shurin SB, Chandrasekaran V, Stabler SP, Sabio H, Bouhassira EE, Upshaw JD Jr, Ginsburg D, Tsai HM. Mutations in a member of the ADAMTS gene family cause thrombotic thrombocytopenic purpura. *Nature* 2001; **413**: 488–94.
7 Zheng X, Chung D, Takayama TK, Majerus EM, Sadler JE, Fujikawa K. Structure of von Willebrand factor-cleaving protease (ADAMTS13), a metalloprotease involved in thrombotic thrombocytopenic purpura. *J Biol Chem* 2001; **276**: 41059–63.
8 Kokame K, Matsumoto M, Soejima K, Yagi H, Ishizashi H, Funato M, Tamai H, Konno M, Kamide K, Kawano Y, Miyata T, Fujimura Y. Mutations and common polymorphisms in ADAMTS13 gene responsible for von Willebrand factor-cleaving protease activity. *Proc Natl Acad Sci USA* 2002; **99**: 11902–7.
9 Lotta LA, Garagiola I, Palla R, Cairo A, Peyvandi F. ADAMTS13 mutations and polymorphisms in congenital thrombotic thrombocytopenic purpura. *Hum Mutat* 2010; **31**: 11–19.
10 Kokame K, Kokubo Y, Miyata T. Polymorphisms and mutations of ADAMTS13 in the Japanese population and estimation of the number of patients with Upshaw–Schulman syndrome. *J Thromb Haemost* 2011; **9**: 1654–6.
11 Jang MJ, Kim NK, Chong SY, Kim HJ, Lee SJ, Kang MS, Oh D. Frequency of Pro475Ser polymorphism of ADAMTS13 gene and its association with ADAMTS-13 activity in the Korean population. *Yonsei Med J* 2008; **49**: 405–8.
12 Gao W, Ruan C, Dai L, Su J, Wang Z. The frequency of P475S polymorphism in von Willebrand factor-cleaving protease in the Chinese population and its relevance to arterial thrombotic disorders. *Thromb Haemost* 2004; **91**: 1257–8.
13 Bongers TN, De Maat MP, Dippel DW, Uitterlinden AG, Leebeek FW. Absence of Pro475Ser polymorphism in ADAMTS-13 in Caucasians. *J Thromb Haemost* 2005; **3**: 805.
14 Kokame K, Miyata T. Genetic defects leading to hereditary thrombotic thrombocytopenic purpura. *Semin Hematol* 2004; **41**: 34–40.
15 Akiyama M, Kokame K, Miyata T. ADAMTS13 P475S polymorphism causes a lowered enzymatic activity and urea lability *in vitro*. *J Thromb Haemost* 2008; **6**: 1830–2.
16 Soejima K, Matsumoto M, Kokame K, Yagi H, Ishizashi H, Maeda H, Nozaki C, Miyata T, Fujimura Y, Nakagaki T. ADAMTS-13 cysteine-rich/spacer domains are functionally essential for von Willebrand factor cleavage. *Blood* 2003; **102**: 3232–7.
17 Zheng X, Nishio K, Majerus EM, Sadler JE. Cleavage of von Willebrand factor requires the spacer domain of the metalloprotease ADAMTS13. *J Biol Chem* 2003; **278**: 30136–41.
18 Akiyama M, Takeda S, Kokame K, Takagi J, Miyata T. Crystal structures of the noncatalytic domains of ADAMTS13 reveal multiple discontinuous exosites for von Willebrand factor. *Proc Natl Acad Sci USA* 2009; **106**: 19274–9.
19 Crawley JT, de Groot R, Xiang Y, Luken BM, Lane DA. Unraveling the scissile bond: how ADAMTS13 recognizes and cleaves von Willebrand factor. *Blood* 2011; **118**: 3212–21.
20 Wu JJ, Fujikawa K, McMullen BA, Chung DW. Characterization of a core binding site for ADAMTS-13 in the A2 domain of von Willebrand factor. *Proc Natl Acad Sci USA* 2006; **103**: 18470–4.
21 Jin SY, Skipwith CG, Zheng XL. Amino acid residues Arg(659), Arg(660), and Tyr(661) in the spacer domain of ADAMTS13 are critical for cleavage of von Willebrand factor. *Blood* 2010; **115**: 2300–10.

22 Pos W, Crawley JT, Fijnheer R, Voorberg J, Lane DA, Luken BM. An autoantibody epitope comprising residues R660, Y661, and Y665 in the ADAMTS13 spacer domain identifies a binding site for the A2 domain of VWF. *Blood* 2010; **115**: 1640–9.
23 Akiyama M, Takeda S, Kokame K, Takagi J, Miyata T. Production, crystallization and preliminary crystallographic analysis of an exosite-containing fragment of human von Willebrand factor-cleaving proteinase ADAMTS13. *Acta Crystallogr F Struct Biol Crystallogr Commun* 2009; **65**: 739–42.
24 Reeves PJ, Callewaert N, Contreras R, Khorana HG. Structure and function in rhodopsin: high-level expression of rhodopsin with restricted and homogeneous *N*-glycosylation by a tetracycline-inducible *N*-acetylglucosaminyltransferase I-negative HEK293S stable mammalian cell line. *Proc Natl Acad Sci USA* 2002; **99**: 13419–24.
25 Winn MD, Ballard CC, Cowtan KD, Dodson EJ, Emsley P, Evans PR, Keegan RM, Krissinel EB, Leslie AG, McCoy A, McNicholas SJ, Murshudov GN, Pannu NS, Potterton EA, Powell HR, Read RJ, Vagin A, Wilson KS. Overview of the CCP4 suite and current developments. *Acta Crystallogr D Biol Crystallogr* 2011; **67**: 235–42.
26 Emsley P, Lohkamp B, Scott WG, Cowtan K. Features and development of Coot. *Acta Crystallogr D Biol Crystallogr* 2010; **66**: 486–501.
27 Brunger AT. Version 1.2 of the crystallography and NMR system. *Nat Protoc* 2007; **2**: 2728–33.
28 Kokame K, Nobe Y, Kokubo Y, Okayama A, Miyata T. FRETS-VWF73, a first fluorogenic substrate for ADAMTS13 assay. *Br J Haematol* 2005; **129**: 93–100.
29 Anderson PJ, Kokame K, Sadler JE. Zinc and calcium ions cooperatively modulate ADAMTS13 activity. *J Biol Chem* 2006; **281**: 850–7.
30 Zhang P, Pan W, Rux AH, Sachais BS, Zheng XL. The cooperative activity between the carboxyl-terminal TSP1 repeats and the CUB domains of ADAMTS13 is crucial for recognition of von Willebrand factor under flow. *Blood* 2007; **110**: 1887–94.
31 De Marco L, Shapiro SS. Properties of human asialo-factor VIII. A ristocetin-independent platelet-aggregating agent. *J Clin Invest* 1981; **68**: 321–8.
32 Gonzalez de Peredo A, Klein D, Macek B, Hess D, Peter-Katalinic J, Hofsteenge J. *C*-mannosylation and *O*-fucosylation of thrombospondin type 1 repeats. *Mol Cell Proteomics* 2002; **1**: 11–18.
33 Wang LW, Leonhard-Melief C, Haltiwanger RS, Apte SS. Post-translational modification of thrombospondin type-1 repeats in ADAMTS-like 1/punctin-1 by *C*-mannosylation of tryptophan. *J Biol Chem* 2009; **284**: 30004–15.
34 Zhang Q, Zhou YF, Zhang CZ, Zhang X, Lu C, Springer TA. Structural specializations of A2, a force-sensing domain in the ultralarge vascular protein von Willebrand factor. *Proc Natl Acad Sci USA* 2009; **106**: 9226–31.
35 Zhang X, Halvorsen K, Zhang CZ, Wong WP, Springer TA. Mechanoenzymatic cleavage of the ultralarge vascular protein von Willebrand factor. *Science* 2009; **324**: 1330–4.
36 Zakai NA, McClure LA. Racial differences in venous thromboembolism. *J Thromb Haemost* 2011; **9**: 1877–82.
37 Miyata T, Hamasaki N, Wada H, Kojima T. More on: racial differences in venous thromboembolism. *J Thromb Haemost* 2012; **10**: 319–20.
38 Zhou W, Bouhassira EE, Tsai HM. An IAP retrotransposon in the mouse ADAMTS13 gene creates ADAMTS13 variant proteins that are less effective in cleaving von Willebrand factor multimers. *Blood* 2007; **110**: 886–93.
39 Kokame K, Matsumoto M, Fujimura Y, Miyata T. VWF73, a region from D1596 to R1668 of von Willebrand factor, provides a minimal substrate for ADAMTS-13. *Blood* 2004; **103**: 607–12.